Author Manuscript

Author Manuscript

Author Manuscript

Author Manuscript

HHS Public Access

Author manuscript

J Surg Res. Author manuscript; available in PMC 2015 May 01.

Published in final edited form as:

J Surg Res. 2014 May 1; 188(1): 119–128. doi:10.1016/j.jss.2013.11.1089.

Use of monoclonal antibody-IRDye800CW bioconjugates in the resection of breast cancer

Melissa L. Korb, MD[a], **Yolanda E. Hartman, BS**[a], **Joy Kovar, MS**[b], **Kurt R. Zinn, PhD, DVM**[c], **Kirby I. Bland, MD**[a], and **Eben L. Rosenthal, MD**[a,*]

[a]Department of Surgery, University of Alabama at Birmingham, Birmingham, Alabama

[b]LI-COR Biosciences, Lincoln, Nebraska

[c]Department of Radiology, University of Alabama at Birmingham, Birmingham, Alabama

Abstract

Background—Complete surgical resection of breast cancer is a powerful determinant of patient outcome, and failure to achieve negative margins results in reoperation in between 30% and 60% of patients. We hypothesize that repurposing Food and Drug Administration approved antibodies as tumor-targeting diagnostic molecules can function as optical contrast agents to identify the boundaries of malignant tissue intraoperatively.

Materials and methods—The monoclonal antibodies bevacizumab, cetuximab, panitumumab, trastuzumab, and tocilizumab were covalently linked to a near-infrared fluorescence probe (IRDye800CW) and in vitro binding assays were performed to confirm ligand-specific binding. Nude mice bearing human breast cancer flank tumors were intravenously injected with the antibody-IRDye800 bioconjugates and imaged over time. Tumor resections were performed using the SPY and Pearl Impulse systems, and the presence or absence of tumor was confirmed by conventional and fluorescence histology.

Results—Tumor was distinguishable from normal tissue using both SPY and Pearl systems, with both platforms being able to detect tumor as small as 0.5 mg. Serial surgical resections demonstrated that real-time fluorescence can differentiate subclinical segments of disease. Pathologic examination of samples by conventional and optical histology using the Odyssey scanner confirmed that the bioconjugates were specific for tumor cells and allowed accurate differentiation of malignant areas from normal tissue.

Conclusions—Human breast cancer tumors can be imaged in vivo with multiple optical imaging platforms using near-infrared fluorescently labeled antibodies. These data support additional preclinical investigations for improving the surgical resection of malignancies with the goal of eventual clinical translation.

Keywords

Antibody; Breast cancer; Fluorescence; Near-infrared; Optical imaging

Corresponding Author: Eben L. Rosenthal, MD, Division of Otolaryngology, BDB Suite 563, 1808 7th Avenue South, Birmingham, AL 35294-0012, Tel: (205) 934-9767, Fax: (205) 934-3993, oto@uab.edu.

This work will be presented at the 2013 American College of Surgeons Clinical Congress in Washington D.C.

Author Manuscript Author Manuscript Author Manuscript Author Manuscript

1. Introduction

Breast conservation surgery (BCS) has become a standard of care for the surgical treatment of early stage breast cancers. However, positive margins (tumor cells present within 2 mm of the surgical margin) after BCS are a significant concern, with a reported incidence of 20% - 60% [1,2]. Of these cases, 15% - 60% result in need for re-excision [3,4]. This exposes patients to additional cost, time, risk of anesthesia, postoperative pain, and poorer cosmetic outcomes. It has also been shown that patients with positive margins have higher rates of breast cancer recurrence [5,6]. Current strategies for intraoperative identification of tumor boundaries and positive margins include wire-guided localization, intraoperative ultrasound-guided resection, intraoperative specimen radiography, cryoprobe-assisted localization, frozen section analysis, intraoperative touch preparation cytology, and standardized surgical cavity shaving; however, the techniques used are not consistent between treatment centers and each modality has limitations, with none being shown to singularly outperform the others [6].

It is with this in mind that near-infrared (NIR) fluorescence technology has become an area of considerable interest for real-time intraoperative evaluation of tumor margins. This technology avoids interference from tissue autofluorescence and allows the assessment beyond the tumor surface by using fluorophores that emit light at 700–900 nm, such as IRDye800CW. For these agents to assist in tumor identification, they require a targeting probe for delivery to the site of disease. Strategies for tumor targeting vary widely, but a promising avenue involves repurposing Food and Drug Administration (FDA) approved monoclonal antibodies as tumor-directed molecules. This technique has been reported in multiple tumor types including head and neck, cutaneous squamous cell, melanoma, ovarian, and breast using preclinical models [7–11]. Potential targets of this therapy include human epidermal growth factor receptor 2 (HER2/neu), vascular endothelial growth factor (VEGF), epidermal growth factor receptor (EGFR), and interleukin 6 receptor (IL-6R), which all have been shown to be overexpressed in breast cancers [9,12–16] and have existing FDA-approved antibodies that are clinically available (trastuzumab, bevacizumab, cetuximab, panitumumab, and tocilizumab). However, a comparison of FDA-approved antibodies for imaging breast cancer has not been performed, thus the relative potential of each agent for clinical translation is unknown.

In addition to tumor-specific delivery of the contrast agent, an appropriate imaging platform must be available for intraoperative tumor visualization. Currently, there are a few FDA approved NIR systems used in the operating room that have the capacity to assist with real-time tumor resection and margin analysis, including the SPY system (Lifecell, Branchburg, NJ). SPY was developed to assess vascular perfusion in cardiac and plastic surgery procedures through the detection of indocyanine green (ICG) [17]. The overlap of the emission and absorption spectra of ICG and IRDye800CW facilitates the potential use of the SPY system in cancer-specific imaging. Considering the FDA approval and general availability of this imaging system, key components for real-time surgical margin assessment using this strategy are currently in place to immediately impact patient treatment.

Author Manuscript Author Manuscript Author Manuscript Author Manuscript

By using devices and therapeutic targeting agents that are currently clinically accessible, we believe the translational potential of this technology is evident. Not only does this technique represent a novel solution to identify positive margins, but it also combines the existing modalities that are safe for patients without significant added cost to treatment facilities.

In this study, we characterize the potential of SPY to detect and assist with the resection of breast tumors using five FDA approved antibody-IRDye800 bioconjugates in a preclinical murine model. This is the first report to simultaneously compare bevacizumab, cetuximab, panitumumab, tocilizumab, and trastuzumab in breast cancer. Additionally, we seek to determine the detection threshold of this technique for identifying subclinical disease.

2. Materials and Methods

2.1. Cell lines and tissue culture

2LMP (2-times lung metastatic pooled) triple-negative human breast cancer cells, derived from MDA-MB-231 (MD Anderson metastatic breast), were obtained from the laboratory of Dr. Donald Buchsbaum at the University of Alabama in Birmingham. Cells were maintained in ulbecco's modified Eagles medium, 10% fetal bovine serum, 1% L-glutamine, and 1% penicillin, streptomycin, and amphotericin B. Cells were incubated at 37C in 5% CO2, and cultured to 80% confluence. Cell number was determined by a hemocytometer and the trypan dye exclusion method, and 2.5–106 cells inphosphate-buffered solution (PBS) were injected subcutaneously on the flank.

2.2. Reagents

The antibodies used were anti-VEGF antibody, bevacizumab (Avastin, Genentech, San Francisco, CA; 149 kDa); anti-EGFR antibody, cetuximab (Erbitux, ImClone, New York, NY; 152 kDa); fully humanized anti-EGFR antibody, panitumumab (Vectibix, Amgen, Thousand Oaks, CA; 147 kDa); anti-IL-6R antibody, tocilizumab (Actemra, Genentech; 148 kDa); and anti-HER2/neu antibody, trastuzumab (Herceptin, Genentech, 148 kDa). Control antibody for daily imaging was protein Aepurified immunoglobulin G (IgG) antibody (Innovative, Novi, MI; Ir-Hu-Gf, #30010BM; 146 kDa). The fluorescent probe used was IRDye800CW (IRDye800CW-N-hydroxysuccinimide ester; LI-COR Biosciences, Lincoln, NE). All antibodies were diluted to 1 mg/mL in PBS and incubated with the IRDye800CW for 2 h at room temperature, according to the manufacturer's protocol. After incubation, any remaining unconjugated dye was removed by desalting column (Pierce, Rockford, IL; Zeba, #89891).

2.3. Western blot analysis

Cells were grown to 80% confluence and collected in lysis buffer (50 mM TriseHCl [pH 7.5], 150 mM NaCl, 1% [vol/vol] NP40, 0.5% [wt/vol] sodium deoxycholate, 1 mM ethylenediaminetetraacetic acid, [EDTA], 0.1% sodium dodecyl sulfate [SDS]) and a protease inhibitor cocktail tablet (Roche Applied Science, Indianapolis, IN) was added. The lysate was collected by centrifugation at 13,400 RPM for 30 min at 4C and the protein concentration was measured by bicinchoninic acid (BCA) protein assay (Thermo Scientific, Rockford, IL). Lysate containing 20 mg of protein was separated by sodium dodecyl

Author Manuscript Author Manuscript Author Manuscript Author Manuscript

sulfateepolyacrylamide gel electrophoresis (SDSPAGE) and transferred to a polyvinylidene difluoride (PVDF) membrane. The membrane was probed with b-actin horseradish peroxidase (HRP) (Santa Cruz, Santa Cruz, CA; 47778) to ensure equal protein loading, followed by blocking with 5% nonfat dry milk and incubation with the primary antibodies: EGFR (Santa Cruz, 71034), HER2/neu (Abcam, Cambridge, MA; 2428), IL-6R (Abcam, 27404), and VEGF (Santa Cruz, 7269). After washing and incubating with HRP-conjugated secondary antibodies (goat anti-mouse IgG [Santa Cruz, 2005] and goat anti-rabbit IgG [Santa Cruz, 2004]), the membrane was washed again and developed with the Amersham enhanced chemiluminescence (ECL) Western blotting detection system (GE healthcare, Buckinghamshire, UK).

2.4. Binding affinity assays

To determine antigen specificity after conjugation to IRDye800CW, binding affinity assays were performed for each antibody. Wells of a 96-well black plate were coated with one of the recombinant proteins EGFR (rhEGFR/Fc Chimera; 400 ng/well/100 mL; 344-ER), HER2/neu (rhErbB2/Fc Chimera; 400 ng/well/100 mL; 1129-ER), IL-6R (rhIL-6Ra; 400 ng/well/100 mL; 227-SR/CF), or VEGF (rhVEGF; 100 ng/well/100 mL; 293-VE/CF) overnight at 4C. Wells were blocked for 1h at room temperature with 1% bovine serum albumin. For control, purified antibody (bevacizumab, cetuximab, panitumumab, tocilizumab, or trastuzumab) was added to three lanes of coated wells and allowed to block for 1 h at room temperature. Serial dilutions of the labeled antibody (0.234375e30 nM for bevacizumab, tocilizumab, and trastuzumab; 0.05e6.7 nM for cetuximab and panitumumab) were then added to coated wells and incubated for 3h at 37C. Empty wells on the same plate were also maintained for background control. After incubation, wells were washed three times with PBS and imaged using the Pearl Impulse system (LI-COR Biosciences). Well intensities were quantified for total binding (unblocked wells) and nonspecific binding (blocked wells) using the Pearl Impulse software version 2.0, and values were transferred to GraphPad Prism version 6 for Windows (GraphPad software, San Diego, CA) for binding affinity analysis.

For identification of which receptors were most strongly expressed by breast cancer, this study was replicated by coating wells with 2LMP cells. One hundred microlitres of cells suspended in media were aliquoted into six lanes of a 96-well black plate and allowed to grow to 90%e100% confluence. Purified antibody (bevacizumab, cetuximab, panitumumab, tocilizumab, or trastuzumab) was added to three lanes of coated wells and allowed to block for 1 h at 37C. Serial dilutions of labeled antibody (reference dilution concentrations in previous paragraph) were then added to all coated wells and incubated for 3 h at 37C. After incubation, cells were washed with PBS and imaged using the Pearl.

2.5. Animal models

Nude (nu/nu) female mice (Charles River Laboratories, Hartford, CT), aged 4–6 wk, were purchased and allowed to acclimatize for 1–2 wk before experiments were started. Mice were housed in accordance with the Institutional Animal Care and Use Committee (IACUC) guidelines, and all experiments were conducted and mice were euthanized according to the approved IACUC protocols. All mice received 200 mL subcutaneous injection of 2LMP

Author Manuscript Author Manuscript Author Manuscript Author Manuscript

cells (2.5×10^6) suspended in PBS on either the right or the left flank. Tumors were allowed to grow for 2–3 wk.

To determine if the 2LMP tumors could be visualized and the timing of the peak tumor-to-background ratio (TBR) for each antibody-dye bioconjugate, six mice bearing flank tumors were intravenously injected with one of the five antibody-dye bioconjugates or nonspecific IgG-IRDye800CW for control. The tumors were imaged daily after an injection with the FDA-approved imaging system SPY (Lifecell). Because the SPY was designed to image ICG, findings were confirmed on the preclinical Pearl Impulse system, which was designed specifically to image IRDye800CW. All images were analyzed using Image J software (National Institute of Health, Bethesda, MD). The collection of images continued until the tumors had reached the size limits defined by IACUC and the mice had to be euthanized or the tumor was no longer distinguishable from the background tissues.

For real-time evaluation of tumor margins, 15 mice received tail vein injections of one of the five antibody-dye bioconjugates, and tumor resections were performed on the postinjection day with the highest TBR on SPY as determined by the previous daily imaging experiment. SPY and Pearl systems were used to guide resections and assess the wound bed for any remaining tumor. Samples were then collected from the tumors, the tumor bed, and distant negative control tissue. The samples were imaged with SPY and Pearl in individual imaging cassettes and sent for processing. TBRs were calculated from the SPY and Pearl images.

To evaluate the threshold of detection for each antibody-dye bioconjugate, five mice were intravenously injected with one of the five antibody-dye bioconjugates. Tumor resections were again performed on the postinjection day with the highest TBR on SPY, determined by the previous daily imaging experiment. The skin overlying the tumor was incised to create a flap and the whole tumor was resected and weighed. The whole tumor was then placed back into the wound bed (as an internal control for background fluorescence) and images were collected using SPY and Pearl. Tumors were then dissected in half. One half was discarded and the other was weighed and placed back into the tumor bed for imaging as described previously. The serial sectioning of each tumor proceeded until the tumor could no longer be visualized in the tumor bed by SPY, or the segment could no longer be grossly divided. TBRs were calculated for each image.

2.6. Fluorescent imaging and measurement

Images were captured using the real-time SPY system, with confirmation of fluorescent tissues being performed with Pearl, as previously described [7,10]. The intensity was standardized for all images on the Pearl. SPY images were exported as 8-bit JPEG files and Pearl images were exported as 300 dpi Tiff files. Image J software was used to construct four regions of interest within each tumor and four background regions of interest in the normal tissue adjacent to the tumor. Regions of interest were averaged and TBRs were calculated for each tumor.

2.7. Microscopic fluorescent imaging

Hematoxylin and eosin (H&E)-stained slides were placed in the Odyssey scanner (LI-COR Biosciences) to generate microscopic fluorescent images of a representative tumor section

Author Manuscript Author Manuscript Author Manuscript Author Manuscript

from each antibody-IRDye bioconjugate group. The intensity was standardized for all images. Images were exported as 300 dpi Tiff files.

Higher magnification fluorescence microscopy images were obtained using an Olympus IX81 Inverted Microscope (Olympus, Hamburg, Germany) equipped with a halogen bulb and an NIR filter cube (EXHQ760/40X, 790 dcxr, EMHQ830/50m; Chroma Technology Corp, Rockingham, VT).

2.8. Statistical analysis

Total antibody-IRDye800 bioconjugate binding was compared with nonspecific binding at each dilution for the binding assays using a one-tailed t-test. SPY and Pearl TBR values for each antibody were compared at each time point for the daily imaging of tumors using a one-tailed t-test. For the tumors within the resection group, TBRs for each antibody were compared using a one-way analysis of variance (ANOVA) test. Statistical analysis was performed using GraphPad Prism version 6.0 for Windows (GraphPad Software), and statistical significance was considered at $P < 0.05$.

3. Results

3.1. Antibody-IRdy-800 bioconjugate specificity for imaging breast cancer

Binding assays performed with recombinant protein-coated plates determined that each antibody maintained antigen specificity after IRDye800CW labeling with the binding affinity of each bioconjugate approaching that of the unconjugated antibody. The total binding and nonspecific binding of each labeled antibody was assessed over a range of concentrations, as shown in Figure 1B–F. Given that the nonspecific binding of each antibody-IRDy-800 bioconjugate was very low for each assay, it can be assumed that the total binding curves actually reflect the specific binding of the bioconjugates. There was a statistically significant difference between the total (specific) binding and nonspecific binding for each concentration point on all assays ($P < 0.05$).

To determine ligand expression in our experimental model, 2LMP cell lysates were assessed by Western blotting. Protein levels of EGFR showed the strongest expression, followed by HER2/neu, VEGF, and IL-6R, respectively (Fig. 1A). These data were confirmed by in vitro cell binding assays. Anti-EGFR antibodies (cetuximab and panitumumab) had the strongest uptake of the antibody-dye bioconjugate, whereas the cells treated with anti-VEGF antibody (bevacizumab), anti- IL-6R antibody (tocilizumab), and anti-HER2neu antibody (trastuzumab) showed relatively weak antibody-dye bioconjugate binding (data not shown).

3.2. NIR fluorescent imaging of tumors

Daily imaging of the 2LMP tumors after a single administration of antibody-dye bioconjugate showed that peak TBRs for SPY occurred between 6 and 9 d postinjection and for Pearl occurred between 13 and 16 d (Fig. 2). Additionally, both modalities were able to visualize the tumors for >2 wk after systemic administration. The EGFR-targeting antibodies performed better than the others, with panitumumab achieving peak TBRs of 3.6 using the SPY and 9.8 using the Pearl and cetuximab achieving peak TBRs of 3.2 (SPY) and

Author Manuscript Author Manuscript Author Manuscript Author Manuscript

5.2 (Pearl). A statistically significant difference ($P < 0.05$) was noted between the SPY and Pearl TBR values for panitumumab from day 3 forward and for cetuximab at every time point except day 6 when the SPY and Pearl values crossed. Peak TBRs were 3.1 (SPY) and 3.7 (Pearl) for bevacizumab and 1.9 (SPY) and 2.9 (Pearl) for trastuzumab. A statistically significant difference ($P < 0.05$) was noted between the SPY and Pearl TBR values for bevacizumab from day 5 forward and for trastuzumab at every time point except day 5 when the SPY values were near their peak. Tocilizumab (anti-IL-6R antibody), however, achieved peak TBRs on SPY and Pearl of only 1.4 and 2.6, which were equivalent to the control, nonspecific IgG (1.6 on SPY and 2.4 on Pearl). A statistically significant difference ($P < 0.05$) was noted between the SPY and Pearl TBR values for tocilizumab from day 6 forward and for IgG from day 4 forward.

3.3. NIR fluorescence-guided resection of tumors

After the skin overlying the tumor was removed, tumors were imaged in situ first with SPY, and then with Pearl to confirm the fluorescent findings on SPY. TBRs were, again, highest for the EGFR agents panitumumab (6.8 SPY, 10.9 Pearl) and cetuximab (4.3 SPY, 4.9 Pearl). On SPY imaging, TBRs for both panitumumab and cetuximab were significantly different from each of the other antibodies, and the TBR of panitumumab was significantly better compared with all other antibodies on Pearl imaging. TBRs for the other antibodies, trastuzumab (2.4 SPY, 4.0 Pearl), tocilizumab (2.6 SPY, 3.6 Pearl), and bevacizumab (2.0 SPY, 2.6 Pearl), were all very similar and were not significantly different from each other (Fig. 3).

None of the tumors were noted to be locally invasive or metastatic by imaging. Imaging with SPY and Pearl after tumor resection confirmed complete removal of the malignant tissue.

3.4. Fluorescent confirmation of tumor and intratumoral localization of IRDye

Images of hematoxylin and eosin-stained tumor slides obtained by fluorescence histology using the Odyssey scanner showed that areas of high fluorescence colocalized with histologic evidence of tumor, whereas peripheral regions of benign tissue had low background fluorescence (Fig. 4). Higher magnification inspection of tumor samples with an NIR filter fitted microscope revealed that cetuximab, panitumumab, tocilizumab, and trastuzumab bioconjugates were concentrated within the cytoplasm of tumor cells. The bevacizumab bioconjugate, however, was found within the extracellular matrix of the tumor (Fig. 4).

3.5. Determination of detection threshold for NIR fluorescent imaging

The threshold for microscopic fluorescent immunoguided neoplasm detection has previously been described as the presence of at least 500 malignant cells (0.5 mm tumor) [18]. However, these studies used a stereomicroscope to image the single contrast agent cetuximab-Cy5.5, whereas our study used five separate antibody-IRDye800CW bioconjugates with SPY and Pearl imaging technologies to examine gross tissue. To quantify the tumor burden necessary for imaging the IRDye800CW-conjugated antibodies with SPY and Pearl, we used a serial tumor-sectioning model.

Author Manuscript Author Manuscript Author Manuscript Author Manuscript

The EGFR agent panitumumab achieved the best visualization by identifying the smallest tumor sections within the wound bed, which is consistent with the findings in the aforementioned studies. Figure 5 outlines the SPY and Pearl imaging data obtained using panitumumab IRDye800, which detected tumor fragment weighing just 0.5 mg.

The second most sensitive agent was cetuximab, able to perceive 1.7 mg of tissue, followed by tocilizumab with 2.0 mg of tissue, trastuzumab with 3.4 mg of tissue, and bevacizumab with 4.5 mg of tissue.

4. Discussion

Positive margins after BCS remain a significant issue in the treatment of breast cancer. Current intraoperative evaluation relies on the visual inspection by the surgeon and frozen section analysis, both of which are fairly insensitive [6]. Image-guided surgery with fluorescence-labeled tumor-targeting molecules is a simple, safe adjunct to current practice, which allows for margin assessment at the time of operation.

In this study, we illustrate that among the five FDA approved monoclonal antibodies, the anti-EGFR agents cetuximab and panitumumab proved to be the best for imaging our models. These antibodies conjugated to IRDye800 consistently gave the highest TBRs and allowed the longest duration of tumor visualization after their administration. In fact, the TBRs achieved in our studies are comparable with or greater than those shown by previous investigations [9,19,20]. Additionally, the TBRs for both panitumumab and cetuximab were significantly different from each of the other antibodies on SPY imaging, and the TBR of panitumumab was significantly different compared with all other antibodies on Pearl imaging. Bevacizumab (anti-VEGF) and trastuzumab (anti-HER2/neu) did not show significant uptake in the cell-based binding assay; however, there was strong intratumoral accumulation of these agents in vivo leading to good tumor visualization. For bevacizumab, this discrepancy can likely be explained by differences between the in vitro and in vivo environments, particularly the lack of vascularity in vitro that would lead to VEGF expression. This also explains why the bevacizumab staining in Figure 4 was found extracellularly.

For trastuzumab, this difference can be accounted for by the inconsistent nature of the (low-level) expression of HER2/neu within this cell line. The ability of this modality to image trastuzumab in these triple-negative breast tumors also points to an interesting finding: that receptor overexpression is not necessary for imaging to be possible, but rather that a receptor is simply present. We also discovered that although tocilizumab (anti-IL-6R) can be used to image breast cancer, it provided some of the weakest TBRs secondary to high background signals from nonspecific tissue uptake and unbound bioconjugates remaining in circulation at the time of imaging. This nonspecific uptake was similar to that demonstrated by the control agent IgG-IRDye800 in the daily imaging study. Finally, we were able to demonstrate that using panitumumab-IRDye800 allowed tumor fragments as small as 0.5 mg to be visualized. On the basis of the conversion, 1 g of tissue is equivalent to 1×10^9 cells [21], SPY and Pearl modalities are sensitive to just 500,000 malignant cells. This

Author Manuscript Author Manuscript Author Manuscript Author Manuscript

ability to accurately identify tumor borders curtails the need to blindly remove nonmalignant tissue in an effort to gain negative margins, thus leading to better cosmetic outcomes.

Although many reports agree that the use of monoclonal antibodies carries great potential for clinical translation given their established pharmacokinetics and safety in humans, Woburn, MA), and Pearl Impulse (LI-COR Biosciences) [9,18,26–29]. The significant limitation to each of these modalities is that they are all small-animal imaging devices which are impractical in the real-time imaging of tumors in humans. For this reason, our group has chosen to focus on the SPY System for NIR imaging. Given that SPY is not designed to image IRDye800, we imaged in parallel with the Pearl Impulse system to confirm data obtained by SPY. The Pearl did provide larger TBRs in our models, likely because it was designed to image IRDye800, but did not confer a large advantage over SPY imaging. In the clinical setting, we propose that the SPY camera would be used in the operative resection of tumors, and the Pearl would be used for specimen imaging to aid the surgeon or pathologist in the margin assessment of the removed samples. Furthermore, Pearl could be used to guide the pathologist to the area(s) of a large specimen, a group of lymph nodes, or a tumor margin that should be examined closely for tumor based on the fluorescence intensity in that area. The Odyssey scanner, as demonstrated in our study, could also be used for histopathologic fluorescent histology evaluation. To this end, use of the FDA-approved device, SPY, confers additional translational potential to our technique.

Although we feel that our approach provides a reasonable solution to address positive margin rates, it is not without limitations. Breast cancer represents an extremely heterogeneous group of lesions with variable receptor expression [30,31]. Furthermore, it has been documented that primary lesion characteristics are frequently different from their metastatic counterparts [32]. Although this article used only a single triple-negative breast cancer cell line to demonstrate the efficacy of monoclonal antibodies as tumor-targeting agents, this technique has been verified in multiple breast cancer cell lines in other preclinical studies [11]. This lends evidence to the conclusion that this technique is broadly applicable to many subtypes of breast cancer. Another approach to detect this heterogeneous group of cancers with optical imaging may require targeting multiple antigens using a combination of antibody-IRDye800 bioconjugates. This cocktail of agents could include bioconjugates that accumulate intracellularly (anti-EGFR) as well as extracellularly (anti-VEGF), and could greatly improve tumor visibility. Another concern surrounds the ability of this technique to label ductal carcinoma in situ (DCIS), which is frequently present at the site of positive margins. It has been shown that EGFR and HER2/neu, in particular, are expressed in DCIS at a rate of 48%-60% and 40%-67%, respectively [14,33,34]. This leads us to believe that the ability to accurately detect DCIS with this method is promising. Finally, no performance standard currently exists for the Pearl or Odyssey devices [35]. The result is that a user can adjust the scaling of an image so that the contrast between the diseased and non-diseased tissue is nonexistent, therefore decreasing the sensitivity of this technique. For the purposes of our study, the scaling of all Pearl and Odyssey images was set to the same level. To address alterations in scaling between images, future investigations should involve the use of standards within the field of view for each image. Unknown tissues could then be compared with known tumor positive tissue and known tumor-negative tissue within a single image, and fluorescence values above two standard deviations from

Author Manuscript Author Manuscript Author Manuscript Author Manuscript

negative, for example, would be classified as positive. This suggestion represents a viable solution to this problem; however, before late-stage clinical trials, the development of industry-wide standards is crucial.

5. Conclusions

In brief, monoclonal antibodies conjugated to the NIR probe IRDye800CW are a novel, practical approach to optical imaging in breast cancer surgery. The use of FDA-approved agents and devices makes this method highly translational.

Acknowledgments

The authors would like to thank Dr Andra Frost in the UAB Department of Pathology for her assistance in histology evaluation of study tissues. This work was supported by grants from the NIH (T32CA091078-11) and NIDCR (R21DE019232). Equipment was donated by Novadaq and IRDye800CW was donated by LICOR Biosciences.

References

1. Au GH, Shih WY, Shih WH, et al. Assessing breast cancer margins ex vivo using aqueous quantum-dot-molecular probes. Int J Surg Oncol. 2012; 2012:861257. [PubMed: 23320158]
2. Ruidiaz ME, Blair SL, Kummel AC, Wang-Rodriguez J. Computerized decision support system for intraoperative analysis of margin status in breast conservation therapy. ISRN Surg. 2012; 2012:546721. [PubMed: 23213570]
3. Jung W, Kang E, Kim SM, et al. Factors associated with re-excision after breast-conserving surgery for early-stage breast cancer. J Breast Cancer. 2012; 15:412. [PubMed: 23346170]
4. Yu CC, Chiang KC, Kuo WL, Shen SC, Lo YF, Chen SC. Low re-excision rate for positive margins in patients treated with ultrasound-guided breast-conserving surgery. Breast. 2013; 22:698. [PubMed: 23333255]
5. Dunne C, Burke JP, Morrow M, Kell MR. Effect of margin status on local recurrence after breast conservation and radiation therapy for ductal carcinoma in situ. J Clin Oncol. 2009; 27:1615. [PubMed: 19255332]
6. Pleijhuis RG, Graafland M, de Vries J, Bart J, de Jong JS, van Dam GM. Obtaining adequate surgical margins in breast-conserving therapy for patients with early-stage breast cancer: current modalities and future directions. Ann Surg Oncol. 2009; 16:2717. [PubMed: 19609829]
7. Heath CH, Deep NL, Sweeny L, Zinn KR, Rosenthal EL. Use of panitumumab-IRDye800 to image microscopic head and neck cancer in an orthotopic surgical model. Ann Surg Oncol. 2012; 19:3879. [PubMed: 22669455]
8. Day KE, Beck LN, Heath CH, Huang CC, Zinn KR, Rosenthal EL. Identification of the optimal therapeutic antibody for fluorescent imaging of cutaneous squamous cell carcinoma. Cancer Biol Ther. 2013; 14:271. [PubMed: 23298904]
9. Terwisscha van Scheltinga AG, van Dam GM, Nagengast WB, et al. Intraoperative near-infrared fluorescence tumor imaging with vascular endothelial growth factor and human epidermal growth factor receptor 2 targeting antibodies. J Nucl Med. 2011; 52:1778. [PubMed: 21990576]
10. Day KE, Beck LN, Deep NL, Kovar J, Zinn KR, Rosenthal EL. Fluorescently labeled therapeutic antibodies for detection of microscopic melanoma. Laryngoscope. 2013; 123:2681. [PubMed: 23616260]
11. Kijanka M, Warnders FJ, El Khattabi M, et al. Rapid optical imaging of human breast tumour xenografts using anti-HER2 VHHs site-directly conjugated to IRDye 800CW for image-guided surgery. Eur J Nucl Med Mol Imaging. 2013; 40:1718. [PubMed: 23778558]
12. Backer MV, Levashova Z, Patel V, et al. Molecular imaging of VEGF receptors in angiogenic vasculature with single-chain VEGF-based probes. Nat Med. 2007; 13:504. [PubMed: 17351626]

Author Manuscript Author Manuscript Author Manuscript Author Manuscript

13. Anderson CJ, Ferdani R. Copper-64 radiopharmaceuticals for PET imaging of cancer: advances in preclinical and clinical research. Cancer Biother Radiopharm. 2009; 24:379. [PubMed: 19694573]
14. Suo Z, Bjaamer A, Ottestad L, Nesland JM. Expression of EGFR family and steroid hormone receptors in ductal carcinoma in situ of the breast. Ultrastruct Pathol. 2001; 25:349. [PubMed: 11758715]
15. Tang P, Wang X, Schiffhauer L, et al. Expression patterns of ER-alpha, PR, HER-2/neu, and EGFR in different cell origin subtypes of high grade and non-high grade ductal carcinoma in situ. Ann Clin Lab Sci. 2006; 36:137. [PubMed: 16682508]
16. Garcia-Tunon I, Ricote M, Ruiz A, Fraile B, Paniagua R, Royuela M. IL-6, its receptors and its relationship with bcl-2 and bax proteins in infiltrating and in situ human breast carcinoma. Histopathology. 2005; 47:82. [PubMed: 15982327]
17. Gurtner GC, Jones GE, Neligan PC, et al. Intraoperative laser angiography using the SPY system: review of the literature and recommendations for use. Ann Surg Innov Res. 2013; 7:1. [PubMed: 23289664]
18. Kulbersh BD, Duncan RD, Magnuson JS, Skipper JB, Zinn K, Rosenthal EL. Sensitivity and specificity of fluorescent immunoguided neoplasm detection in head and neck cancer xenografts. Arch Otolaryngol Head Neck Surg. 2007; 133:511. [PubMed: 17520766]
19. Vermeulen JF, van Brussel AS, Adams A, et al. Near-infrared fluorescence molecular imaging of ductal carcinoma in situ with CD44v6-specific antibodies in mice: a preclinical study. Mol Imaging Biol. 2013; 15:290. [PubMed: 23184608]
20. Keereweer S, Mol IM, Vahrmeijer AL, et al. Dual wavelength tumor targeting for detection of hypopharyngeal cancer using near-infrared optical imaging in an animal model. Int J Cancer. 2012; 131:1633. [PubMed: 22234729]
21. Kim H, Chaudhuri TR, Buchsbaum DJ, Wang D, Zinn KR. High-resolution single-photon emission computed tomography and X-ray computed tomography imaging of Tc-99m-labeled anti-DR5 antibody in breast tumor xenografts. Mol Cancer Ther. 2007; 6:866. [PubMed: 17363481]
22. Adams KE, Ke S, Kwon S, et al. Comparison of visible and near-infrared wavelength-excitable fluorescent dyes for molecular imaging of cancer. J Biomed Opt. 2007; 12:024017. [PubMed: 17477732]
23. Tanaka E, Choi HS, Fujii H, Bawendi MG, Frangioni JV. Image-guided oncologic surgery using invisible light: completed pre-clinical development for sentinel lymph node mapping. Ann Surg Oncol. 2006; 13:1671. [PubMed: 17009138]
24. Marshall MV, Draney D, Sevick-Muraca EM, Olive DM. Single-dose intravenous toxicity study of IRDye 800CW in Sprague-Dawley rats. Mol Imaging Biol. 2010; 12:583. [PubMed: 20376568]
25. Sano K, Nakajima T, Miyazaki K, et al. Short PEG-linkers improve the performance of targeted, activatable monoclonal antibody-indocyanine green optical imaging probes. Bioconjug Chem. 2013; 24:811. [PubMed: 23600922]
26. Rosenthal EL, Kulbersh BD, Duncan RD, et al. In vivo detection of head and neck cancer orthotopic xenografts by immunofluorescence. Laryngoscope. 2006; 116:1636. [PubMed: 16954995]
27. Gleysteen JP, Newman JR, Chhieng D, Frost A, Zinn KR, Rosenthal EL. Fluorescent labeled anti-EGFR antibody for identification of regional and distant metastasis in a preclinical xenograft model. Head Neck. 2008; 30:782. [PubMed: 18228526]
28. Gleysteen JP, Duncan RD, Magnuson JS, Skipper JB, Zinn K, Rosenthal EL. Fluorescently labeled cetuximab to evaluate head and neck cancer response to treatment. Cancer Biol Ther. 2007; 6:1181. [PubMed: 17637562]
29. Sano K, Mitsunaga M, Nakajima T, Choyke PL, Kobayashi H. In vivo breast cancer characterization imaging using two monoclonal antibodies activatably labeled with near infrared fluorophores. Breast Cancer Res. 2012; 14:R61. [PubMed: 22510481]
30. Montagna E, Maisonneuve P, Rotmensz N, et al. Heterogeneity of triple-negative breast cancer: histologic subtyping to inform the outcome. Clin Breast Cancer. 2013; 13:31. [PubMed: 23098574]

Author Manuscript Author Manuscript Author Manuscript Author Manuscript

31. Patchefsky AS, Schwartz GF, Finkelstein SD, et al. Heterogeneity of intraductal carcinoma of the breast. Cancer. 1989; 63:731. [PubMed: 2536585]
32. Ibrahim T, Farolfi A, Scarpi E, et al. Hormonal receptor, human epidermal growth factor receptor-2, and Ki67 discordance between primary breast cancer and paired metastases: clinical impact. Oncology. 2013; 84:150. [PubMed: 23257904]
33. Kommoss F, Colley M, Hart CE, Franklin WA. In situ distribution of oncogene products and growth factor receptors in breast carcinoma: c-erbB-2 oncoprotein, EGFr, and PDGFr-beta-subunit. Mol Cell Probes. 1990; 4:11. [PubMed: 1969111]
34. Somerville JE, Clarke LA, Biggart JD. c-erbB-2 overexpression and histological type of in situ and invasive breast carcinoma. J Clin Pathol. 1992; 45:16. [PubMed: 1346789]
35. Sevick-Muraca EM, Zhu B. The need for performance standards in clinical translation and adoption of fluorescence molecular imaging. Med Phys. 2013; 40:040402. [PubMed: 23556867]

Author Manuscript Author Manuscript Author Manuscript Author Manuscript

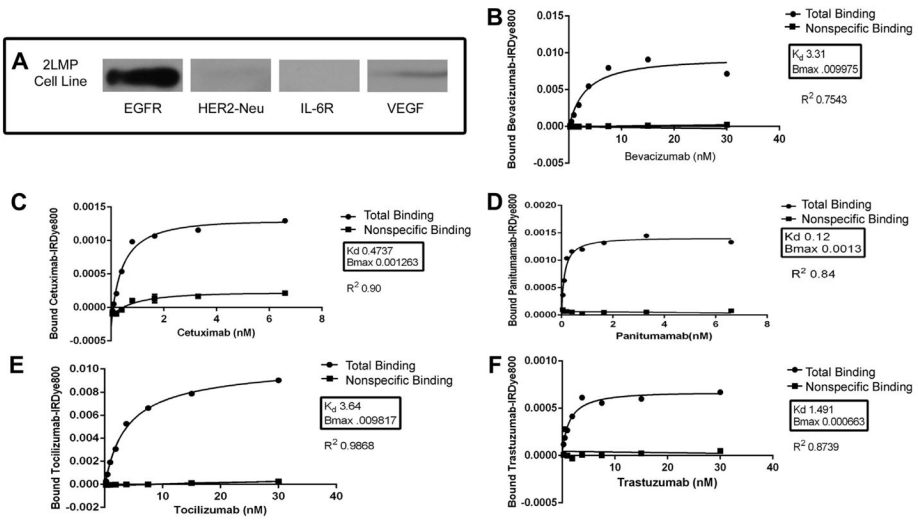

Fig. 1.

(A) Western blot of 2LMP receptor expression. EGFR was the most strongly expressed within the 2LMP cell line. VEGF showed moderate expression, HER2/neu had low-level expression, and IL-6R expression was not demonstrated. (B–F) Antigen binding assays. Nonlinear regression curves demonstrating preservation of antigen specificity after conjugation to IRDye800 for bevacizumab (Avastin), anti-VEGF (B); cetuximab (Erbitux), anti-EGFR (C); panitumumab (Vectibix), anti-EGFR (D); tocilizumab (Actemra), anti-IL-6R (E); and trastuzumab (Herceptin), anti-HER2/neu (F).

Author Manuscript Author Manuscript Author Manuscript Author Manuscript

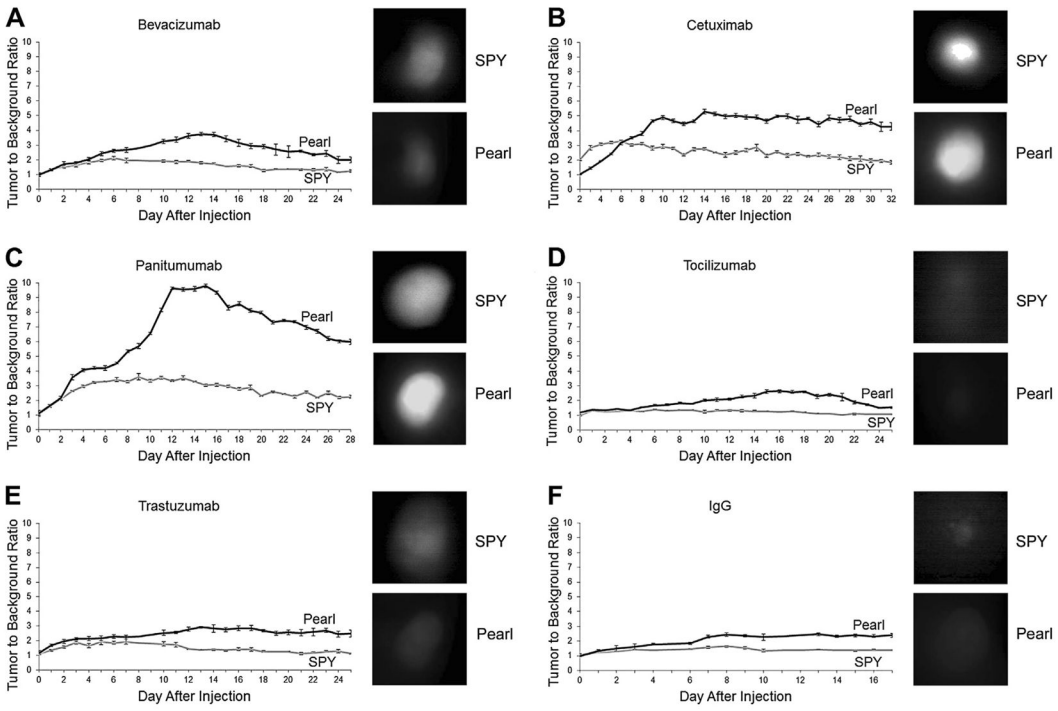

Fig. 2.

(A–F) Daily imaging of tumors. 2LMP flank tumors were imaged daily with both SPY and Pearl modalities. TBRs peaked at 6–9 d on SPY and 13–16 d on Pearl. SPY and Pearl images from the day of peak TBR on each modality are shown adjacent to the TBR graphs for the antibody-IRDye800 bioconjugates. Cetuximab and panitumumab provided the highest TBR. Tocilizumab provided the TBR similar to control IgG. Error bars indicate the standard deviation. (Color version of figure is available online.)

Author Manuscript Author Manuscript Author Manuscript Author Manuscript

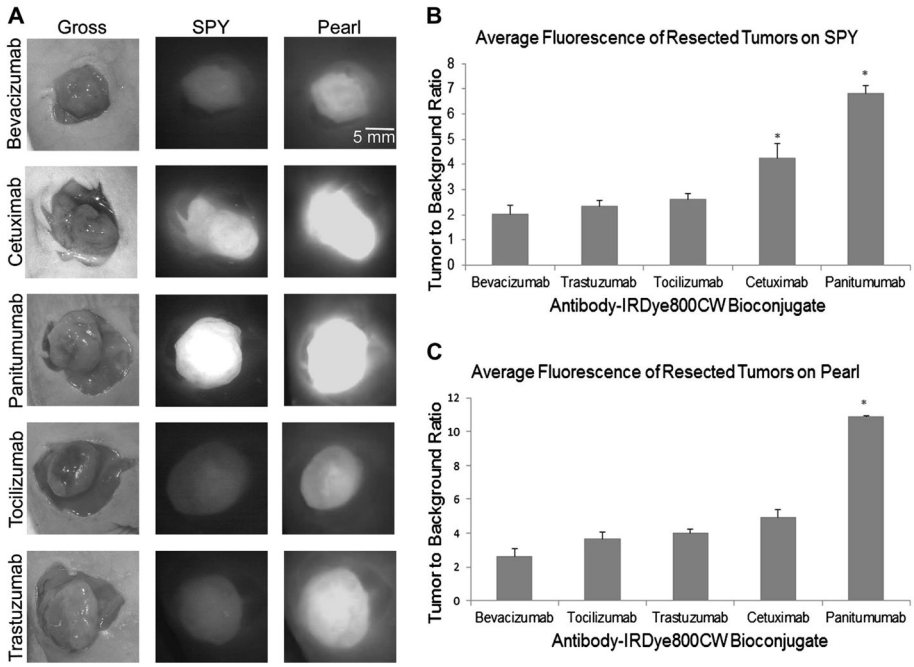

Fig. 3.

(A) Uptake of antibody-IRDye800 within 2LMP flank tumors at the time of resection. Surgical resections were performed in real-time with SPY and confirmed with Pearl. (B and C) TBRs for resected tumors on SPY and Pearl. Cetuximab and panitumumab gave the highest TBR on both modalities. Error bars indicate the standard error. *Significance at $P<0.05$. (Color version of figure is available online.)

Author Manuscript Author Manuscript Author Manuscript Author Manuscript

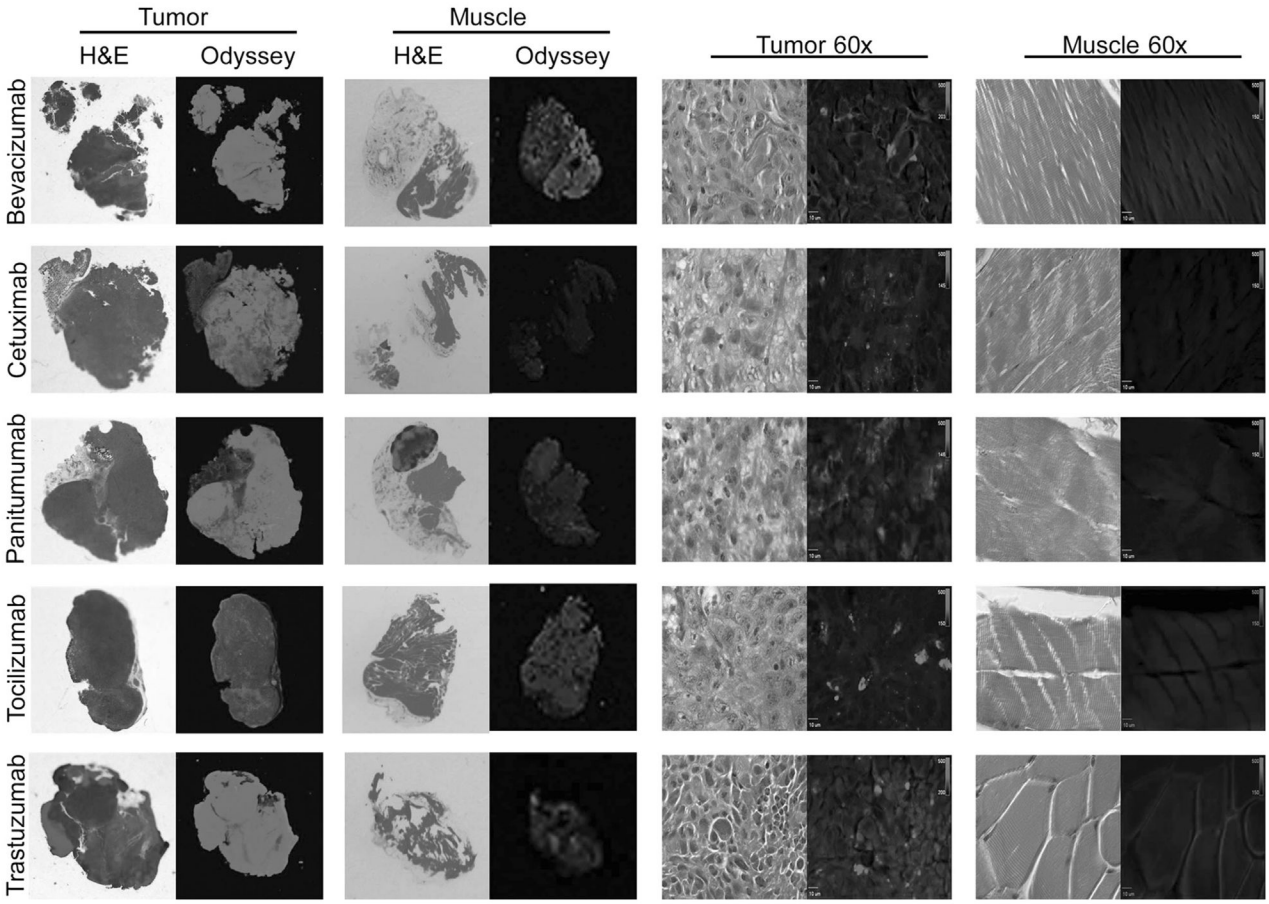

Fig. 4.

Traditional hematoxylin and eosin and fluorescent microscopy of 2LMP tumors and normal tissue (muscle). Odyssey images permit distinction between neoplastic tissue and normal tissue based on the fluorescence intensity. Fluorescent microscopy images (x60) show the pattern of antibodye-IRDye800 uptake within the tumors compared with normal tissue. (Color version of figure is available online.)

Author Manuscript Author Manuscript Author Manuscript Author Manuscript

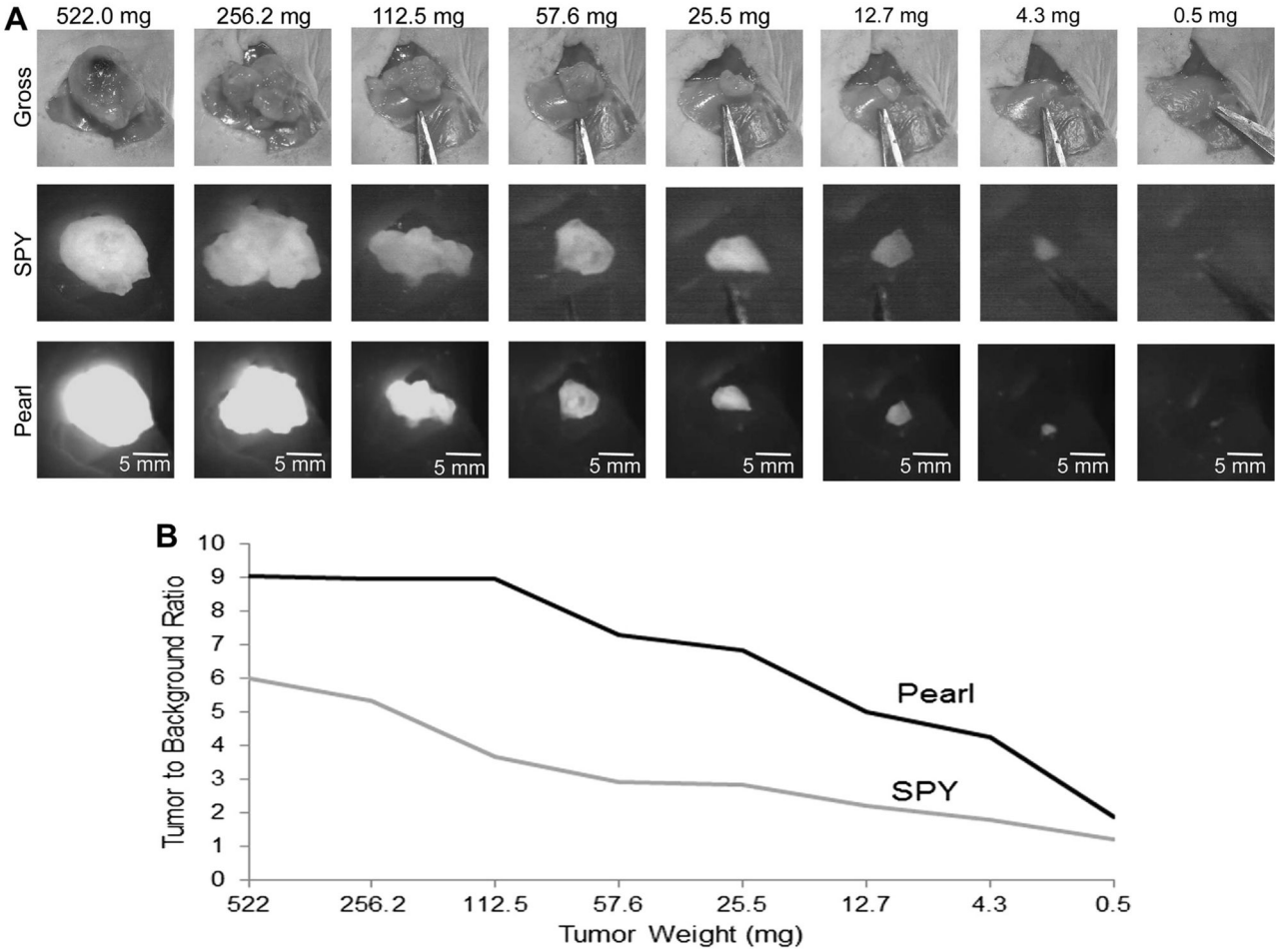

Fig. 5.

(A) Serial tumor resection with panitumumab-IRDye800. Tumor was weighed, imaged, and resected in half until it could no longer be grossly divided. Panitumumab-IRDye800 allowed detection of the smallest fragment of tumor (0.5 mg). Note that tumor was imaged within the tumor bed to account for background fluorescence. (B) TBR of tumor sections by SPY and Pearl. Fluorescence decreased with decreasing tumor size, but was still greater than background with only 0.5 mg of tumor remaining. (Color version of figure is available online.)